pISSN 2508-1888
eISSN 2466-2461
http://dx.doi.org/10.14407/jrpr.2016.41.2.093

Journal of
Radiation Protection and Research

Paper

Received July 17, 2015 / 1st Revised April 24, 2016 / Accepted June 13, 2016

Energy Spectrum Measurement of High Power and High Energy (6 and 9 MeV) Pulsed X-ray Source for Industrial Use

Hiroyuki Takagi*,† and Isao Murata†
*Hitachi, Ltd. Power Systems Company, Ibaraki, Japan
†Graduate School of Engineering, Osaka University, Osaka, Japan

ABSTRACT

Background: Industrial X-ray CT system is normally applied to non-destructive testing (NDT) for industrial product made from metal. Furthermore there are some special CT systems, which have an ability to inspect nuclear fuel assemblies or rocket motors, using high power and high energy (more than 6 MeV) pulsed X-ray source. In these case, pulsed X-ray are produced by the electron linear accelerator, and a huge number of photons with a wide energy spectrum are produced within a very short period. Consequently, it is difficult to measure the X-ray energy spectrum for such accelerator-based X-ray sources using simple spectrometry. Due to this difficulty, unexpected images and artifacts which lead to incorrect density information and dimensions of specimens cannot be avoided in CT images. For getting highly precise CT images, it is important to know the precise energy spectrum of emitted X-rays.

Materials and Methods: In order to realize it we investigated a new approach utilizing the Bayesian estimation method combined with an attenuation curve measurement using step shaped attenuation material. This method was validated by precise measurement of energy spectrum from a 1 MeV electron accelerator. In this study, to extend the applicable X-ray energy range we tried to measure energy spectra of X-ray sources from 6 and 9 MeV linear accelerators by using the recently developed method.

Results and Discussion: In this study, an attenuation curves are measured by using a step-shaped attenuation materials of aluminum and steel individually, and the each X-ray spectrum is reconstructed from the measured attenuation curve by the spectrum type Bayesian estimation method.

Conclusion: The obtained result shows good agreement with simulated spectra, and the presently developed technique is adaptable for high energy X-ray source more than 6 MeV.

Correspondence to Hiroyuki Takagi
hiroyuki.takagi.bc@hitachi.com

Keywords: Bayesian estimation, Energy distribution, High energy X-ray, Non-destructive testing, Attenuation curve, accelerator

1. INTRODUCTION

In the case of accelerator-based X-ray sources for industrial computed tomography systems (CTs) to inspect metal and large materials, X-ray energy should be higher and they are produced by electrons with energies of more than 6 MeV. In such X-ray sources, the peak current of the electron beam is more than 100 mA and the pulse width is about 5 μs. (In this paper, X-rays over 6 MeV are called high energy X-rays.) As a result, a huge number of photons with a wide energy spectrum are produced within quite a short time. Consequently, it is difficult to measure the X-ray energy spectrum using simple spectrometry especially for such commercially available accelerator-based X-ray sources. Due to this difficulty, normally unexpected images and artifacts which lead to incorrect density information and dimensions of specimens cannot be avoided in the CT images. For getting more precise CT images, it is important to know the precise energy spectrum of emitted X-rays. Several techniques have been proposed so far, in which X-ray intensities are measured after penetrating through attenuation material in order to estimate the energy spectrum roughly with a wide energy bin width of around 1 MeV or to estimate quite low energy X-rays of less than 100 keV [1-3]. In these cases, the accuracy of the estimated results is still insufficient from the standpoint of engineering for high energy X-ray CT systems up to 9 MeV, because the energy resolution is insufficient, in other words, a fine energy bin width of less than 100 keV is required. In order to know such a precise energy spectrum, we investigated a new approach utilizing the Bayesian estimation method combined with an attenuation curve measurement using step shaped attenuation material. This method was validated by precise measurement of energy spectrum from a 1 MeV electron accelerator [4]. Our purpose in this study is to extend the applicable X-ray energy range. Using the recently developed technique, we measure precise energy spectra of X-ray sources from 6 and 9 MeV linear accelerators with an energy bin width of 100 keV.

2. MATERIALS AND METHODS

2.1 Attenuation curve measurement

According to results obtained with EGS5 [5], a Monte Carlo simulation code, the number density of photons emitted from a linear accelerator for industrial use is more than 1.0×10^6 photons·mm^{-2} at 1 m from the target on the beam center axis for each pulse of 6 MeV electrons. This means that direct measurement of the pulse height spectrum is almost impossible for high energy X-ray source using ordinary X-ray spectrometry.

To realize accurate X-ray energy spectrum measurement, we consider penetration the polychromatic X-rays with energy spectrum, $\phi(E_j)$ [j=1–M], through an attenuation material, the thickness of which can be changed gradually as t_i [i=1–N]. An experimental arrangement for the attenuation curve measurement is shown in Figure 1. An electron linear accelerator of 6 and 9 MeV electrons switchable (Linatron-M, Varian Medical Systems Inc., Palo Alto, CA), with a pulse width of 4.2 μs, is utilized as an X-ray source. At 1 m from the focal spot, the dose rate is 10 Gy·min^{-1} for 6 MeV and 30 Gy·min^{-1} for 9 MeV without a flattening filter in both cases. In the X-ray CT system, there are several hundred of solid state detectors arranged within the 15° fan beam. This enables us to measure multiple attenuation curves within the fan beam at the same time.

In addition, incidence of scattered X-rays is prevented by a multi-hole collimator which is placed in front of the detector array in order to make each detector view only the focal spot. Then, a step-shaped attenuation material made of aluminum or steel is set between the collimator and the X-ray source so as to cover the fan beam. On measurement of 1 MeV X-ray source, we previously applied the attenuation material of aluminum at maximum 300 mm thick with 10 mm step. In this study, the attenuation material is 580 mm thick of aluminum and 290 mm thick of steel respectively at maximum on the center line and it has 58 or 29 steps start from 10 mm to maximum thickness with a 10 mm step. This means that the attenuation material is modified to relatively higher dense material or extended to relatively thicker shape than those of 1 MeV. In the case of the aluminum attenuation material, the obtained attenuation curve has a character of slow attenuation with a lot of measurement data. Normally, sufficient measurement data will support calculating huge matrix equation. On the other hand, the steel attenuation material derives relatively large attenuation and quick attenuation with small number measurement point. Consequently, in this study, we can compare adaptability of slow attenuation and quick attenuation.

By moving the attenuation material, step-by-step, the attenuation curve of each detector from 10 mm to

Corresponding author : Hiroyuki Takagi, hiroyuki.takagi.bc@hitachi.com
1-1, Saiwai-cho 3-chome, Hitachi-shi, Ibaraki-ken, 317-8511 Japan

 http://dx.doi.org/10.14407/jrpr.2016.41.2.093

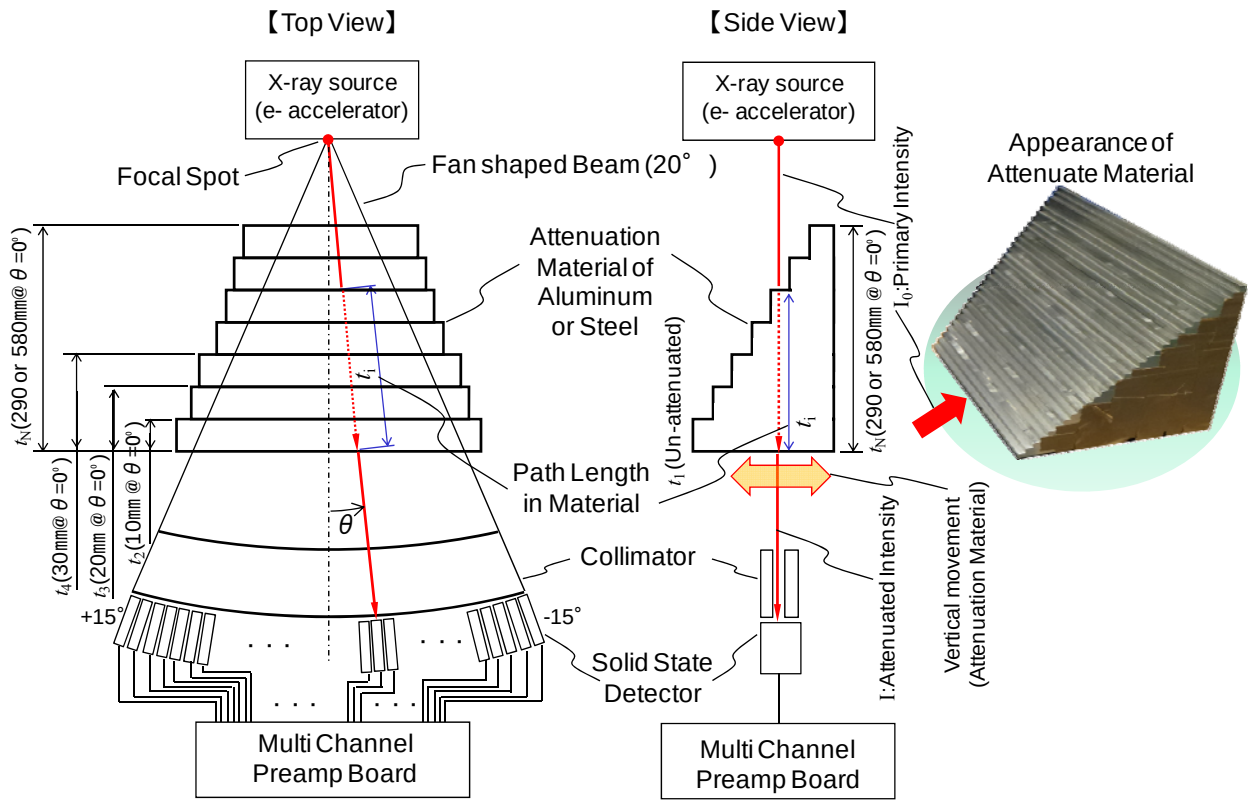

Fig. 1. Experimental setup of array detectors and X-ray source used for the present attenuation curve measurement (The actual path length of the attenuation material is changing according to the angle θ of incident X-rays).

maximum thickness and in addition at 0 mm (with no attenuation material) is obtained. As a result, 59 or 30 X-ray outputs for each detector are recorded separately after penetrating the 59 or 30 steps of the attenuation material by 30 or 59 X-ray irradiations (more than 10,000 pulse per irradiation), that is to say, attenuation curves $y\theta(t_i)$ [$\theta = 0$ to $\pm 15°$, i=1 to 59 or 30], are obtained for all the detectors at the same time.

The path length of X-rays in the attenuation material changes depending on the incident angle θ of the X-rays as shown in Fig. 1. The actual path length is used for t_i in the calculation of energy spectra.

2.2 Spectrum type Bayesian estimation

We use the spectrum type Bayesian estimation method [6] to obtain X-ray energy spectrum $\phi(E_j)$. This method is based on the Bayesian theorem and it has been applied to radiation measurements. For instance, in energy spectrum measurements of charged particles correction of the energy loss in the sample is carried out using the spectrum type Bayesian estimation method as an unfolding technique [7-9]. Furthermore, in X-ray energy spectrum measurement, we recently investigated an approach utilizing the Bayesian estimation method combined with an attenuation curve measurement using step shaped attenuation material. This method was validated by precise measurement of energy spectrum from a 1 MeV electron accelerator. The specific features of the spectrum type Bayesian estimation method are summarized as follows.

(1) Its very simple principle makes for easier application compared to other unfolding methods.
(2) It never gives unfolded results having a negative value.
(3) It does not require any constraint like an initial guess [10].

There should be a quantitative relation between X-ray energy spectrum $\phi(E_j)$ and measured attenuation result $y(t_i)$ for the attenuation curve. It can be described with a response function. The response function $\boldsymbol{H}$ consists of h_{ij} , which includes information on the attenuation coefficient at photon energy E, penetration thickness t_i, and other detector characteristics such as its detection efficiency. This relationship is described as Equation 1.

$$\boldsymbol{y} = \boldsymbol{H} \cdot \boldsymbol{\phi} \tag{1}$$

In the spectrum type Bayesian estimation method, original X-ray spectrum is estimated iteratively carried

out based on Bayes' theorem. The spectrum type Bayesian estimation method deduce the l+1 th estimation $est_j^{(l+1)}(i)$ as,

$$est_j^{(l+1)} = \sum_{i=1}^{N} \left(y(t_i) \times \frac{est_j^{(l)} \times h_{ij}}{\sum_{j=1}^{M} est_j^{(l)} \times h_{ij}} \right) \qquad (2)$$

The above formula is repeatedly used for the measured attenuation curve $y(t_i)$, i.e., a revised $est_j^{(l)}$ is used as the prior information in the next iteration calculation.

2.3 Response function evaluation

In order to estimate the source X-ray energy spectrum, the response function $\boldsymbol{H}$ in eq. 1 is rewritten as $R \cdot \mathrm{F}$ to connect the primary X-ray energy spectrum and the measured pulse height spectrum from preamp board as shown in Fig. 1. Matrix R of N rows and M columns consists of attenuation coefficients varying due to X-ray energy for the column direction and the penetration thickness for the row direction. Matrix F of M rows and M columns contains photon-to-charge conversion factor for the specific X-ray energy induced the detector.

When linear attenuation coefficients μ_j for energies $E_1, E_2, E_3, \ldots, E_M$ as representative energies for energy bins are given, the X-ray energy spectrum $\phi\square(E_j)$ after penetrating through the attenuation material of thickness t_i is taken from the incident X-ray energy spectrum $\phi(E_j)$ and $\exp(-\mu_j \cdot t_i)$. The pulsed X-rays, which penetrated through the attenuation material, are detected and converted into a large electric charge. Generally, the conversion coefficient, that is, the detection efficiency for the X-rays has energy dependence. Now, we define the detection efficiency ε_j for X-ray energy of E_j. The output signal y_i after passing through the attenuation material of thickness t_i is proportional to the value of summarized $\varepsilon_j \cdot \phi\square(E_j)$ with energy bin j from 1 to M .

Applying the energy independent correction factor k to the matrix equation, which depends on the individual measurement system, we express the matrix equation to derive the attenuation curve of X-rays, $y(t_i)$, as in the next equations.

$$\begin{bmatrix} y(t_1) \\ y(t_2) \\ \vdots \\ y(t_N) \end{bmatrix} = k \cdot \begin{bmatrix} \exp(-\mu_1 \cdot t_1) & \exp(-\mu_2 \cdot t_1) & \cdots & \exp(-\mu_M \cdot t_1) \\ \exp(-\mu_1 \cdot t_2) & \exp(-\mu_2 \cdot t_2) & \cdots & \exp(-\mu_M \cdot t_2) \\ \vdots & \vdots & \ddots & \vdots \\ \exp(-\mu_1 \cdot t_N) & \exp(-\mu_2 \cdot t_N) & \cdots & \exp(-\mu_M \cdot t_N) \end{bmatrix} \cdot \begin{bmatrix} \varepsilon_1 & 0 & \cdots & 0 \\ 0 & \varepsilon_2 & \cdots & 0 \\ \vdots & \vdots & \ddots & \vdots \\ 0 & 0 & \cdots & \varepsilon_M \end{bmatrix} \cdot \begin{bmatrix} \phi(E_1) \\ \phi(E_2) \\ \vdots \\ \phi(E_M) \end{bmatrix}$$

$$y = k \cdot R \cdot F \cdot \phi \qquad (3)$$

We describe the evaluation process of the response function $R \cdot F$ in Equation 3 in this section, focusing on a 6 MeV X-ray source and attenuation material of aluminum as an example. The maximum energy of the response function is therefore set to 6 MeV to cover X-rays emitted from the 6 MeV X-ray source. The column of the response function R is then divided into 60 bins, namely they cover the X-ray spectrum from 0.0 to 6.0 MeV with an equal bin width of 0.1 MeV. This means j=1–M (M=60) in Eq. 3. On the other hand, the row component for the attenuation material thickness in Eq. 3 is divided into 59, that is, i=1–N (N=59) as mentioned later in detail. The detection efficiency matrix F is evaluated by calculating the reaction rate of incident monochromatic photons for each energy bin in the actually used detector. The obtained reaction rate is converted into the deposited energy in the detector, i.e., electric charge. We use the Monte Carlo numerical simulation code EGS5 for this evaluation.

The linear attenuation coefficient used in the calculation of the response function R is cited from the data base of the NIST[1].

Finally, in regard to the scalar value of k, because of the dependence on the individual X-ray measurement system, we decide the value experimentally for the system we use.

3. RESULTS AND DISCUSSION

Figure 2 shows attenuation curves in aluminum for 6 and 9 MeV X-ray sources obtained at emission angles of 0° and 15°. The attenuation curves in steel are also shown in Figure 3. The attenuation curves were normalized at zero path length. Both figures show that each curve of emission angle 0° attenuates slower than that of 15° similarly for both X-ray energies. In other words, the energy spectra of 0° contains higher energy photons than 15°. Figures 4 and 5 show X-ray energy spectra, $\phi(E_j)$, estimated from the attenuation curve measurements for 6 MeV and 9 MeV X-ray sources at emission angle of 0°. The spectrum estimation was done with the spectrum type Bayesian estimation method described in chapter 2.2 from the independent measured attenuation curve in Fig. 2 and 3 as y in Eq. 3. As an initial guess a white spectrum was used. The X-ray energy spectrum simulated by the EGS5 code is also shown. In the present simulation, we assumed the tungsten target thickness was

1) X-ray mass attenuation coefficients at NIST. http://physics.nist.gov/PhysRefData/XrayMassCoef/tab4.html

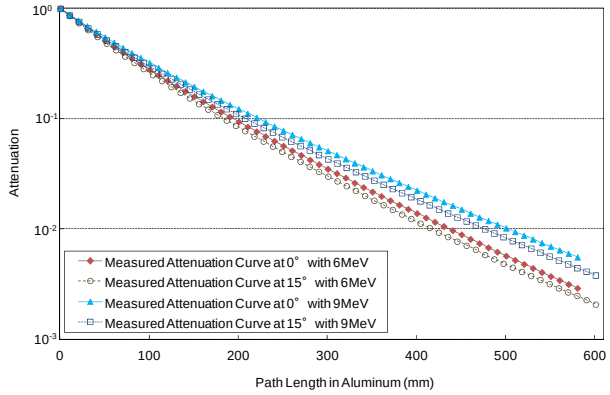

Fig. 2. Measured attenuation curves in aluminum with 6 and 9 MeV X-ray source at emission angles of 0° and 15° (The actual path length of the attenuation material is changing according to the angle θ of incident X-rays as shown in Fig. 1).

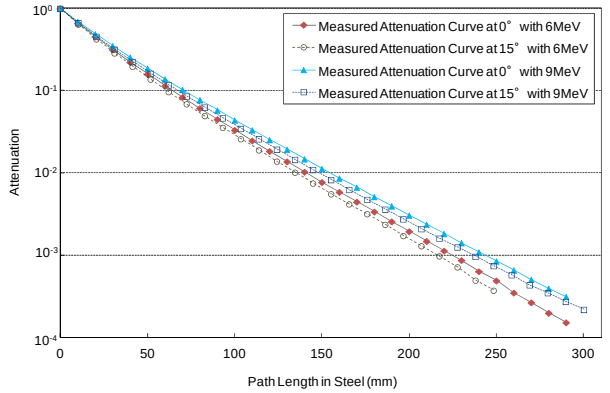

Fig. 3. Measured attenuation curves in steel with 6 and 9 MeV X-ray source at emission angles of 0° and 15° (The actual path length of the attenuation material is changing according to the angle θ of incident X-rays as shown in Fig. 1).

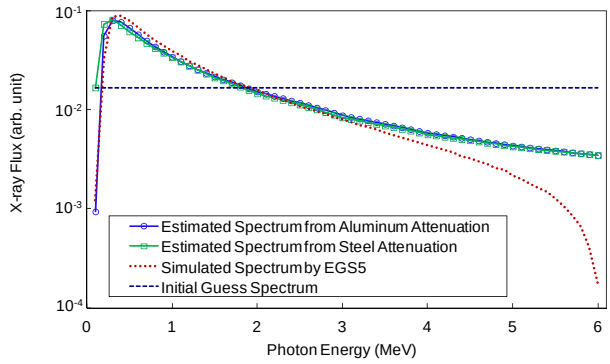

Fig. 4. Measured X-ray energy spectra for 6 MeV X-ray source at emission angles of 0° (normalized to unity).

1 mm. As shown in Fig. 4 and 5, in spite of estimated from independent measured curve, the estimated spectra look quite a similar shape with each other. Furthermore, the experimental spectra are in good agreement with the simulated spectra except for higher energy region more than 4 MeV (for 6 MeV X-ray source) or 6 MeV (for 9 MeV X-ray source). The EGS5 results show smaller values in high energy

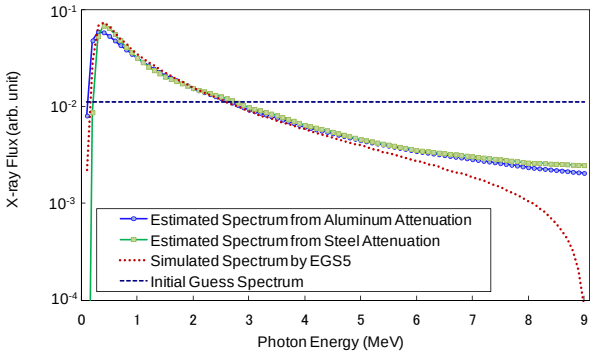

Fig. 5. Measured X-ray energy spectra for 9 MeV X-ray source at emission angles of 0° (normalized to unity).

region compared to the experiment. It is difficult to discuss the reason of this discrepancy. However, it can be said that the present unfolding method based on the Bayes' theorem may not reproduce spectral values having such a small likelihood. Nevertheless, these differences between estimated and simulated spectra at higher energy region are not so serious because those absolute intensities are quite small. Besides, in the present measurement, several hundred attenuation curves $y\theta(t_i)$ within the fan shaped beam of 15° were measured at the same time. This means that a lot of angle-dependent X-ray energy spectra can be measured in the same experiment.

Figures 6 and 7 show measured X-ray energy spectra at typical emission angles of every 5° for 6 MeV and 9 MeV, respectively. These figures show the absolute energy spectra. The vertical axis is the number of photons incident to each detector per pulse. We also note from the figure that the intensity of X-rays decreases with increase of angle θ.

Figures 8 shows the measured average energy for 6 and 9 MeV X-ray sources for each emission angle. Here, the average energy is defined as the energy weighted with the respective normalized spectrum. Each curve shows same trend that the average energy decreases with increase of the emission angle θ. The figure also denotes that all the angular distributions of 9 MeV source show more forward-peeked distributions with respect to emission angle compared to 6 MeV source. This means that higher energy photons are more dominant in forwarder emission angles for both X-ray sources, and the case of 9 MeV shows it more clearly. However, each measured curve is slightly larger than the curve of EGS5 calculation[2)] due to underestimation of EGS5 in higher energy region as mentioned previously.

2) In EGS5 calculation, angular distribution was estimated with a geometry having a finite solid angle to decrease the statistical error. The simulated angular distribution is thus plotted for a finite range of solid angle.

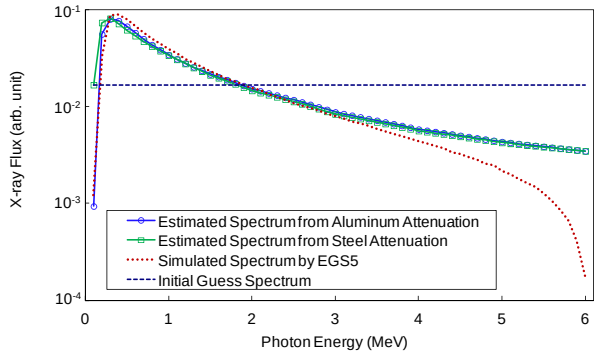

Fig. 6. Measured X-ray energy spectra for 6 MeV X-ray source at emission angles of 0° (normalized to unity).

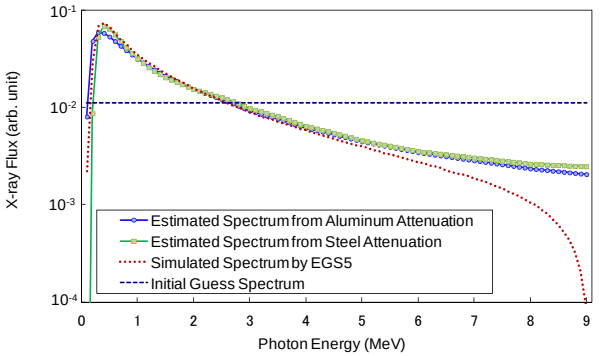

Fig. 7. Measured X-ray energy spectra for 9 MeV X-ray source at emission angles of 0° (normalized to unity).

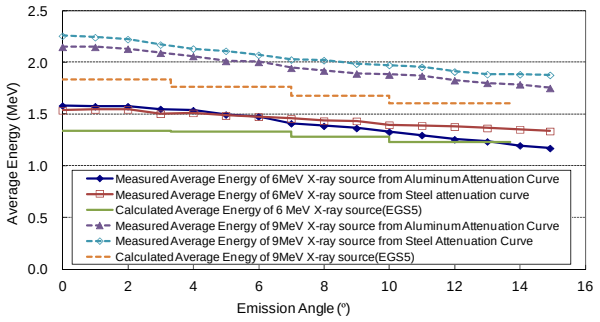

Fig. 8. Average energy of X-rays for 6 and 9 MeV X-ray source for each emission angle.

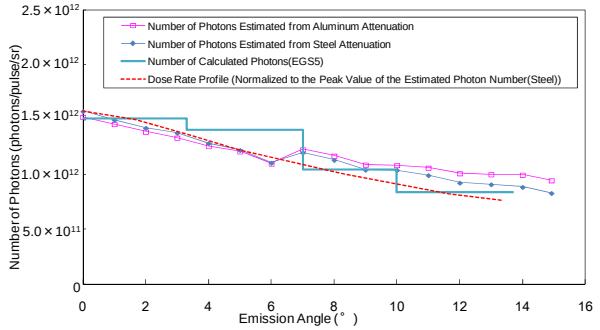

Fig. 9. Total photon number of 6 MeV X-ray source for each emission angle.

Figures 9 and 10 show the angular distributions of the number of photons for 6 and 9 MeV X-ray sources obtained by measurement and the EGS5 simulation. The measured values are derived by integrating the spectra in such as Fig. 6 and 7. The EGS5 simulation result agrees well with the distribution obtained by the present technique. Additionally, dose rate profiles from 6 and 9 MeV X-ray sources measured by a standard air ionization chamber (CC13, IBA Dosimetry GmbH, Schwarzenbruck, Germany) are also shown in Fig. 9 and 10, respectively. Each dose rate profile is normalized to the peak value of the estimated photon number obtained from the case with a steel attenuation. It is notable that the distributions obtained by the ionization chamber and others are in good agreement, though EGS5 simulated distribution might be supported by the distribution of ionization chamber daringly. In any case, distributions obtained by independent attenuation measurements with aluminum and steel are found to be in good agreement with each other. Besides, a forwarder-peaked distribution of 9 MeV source is observed compared to 6 MeV source similar to the angular distribution of average energy.

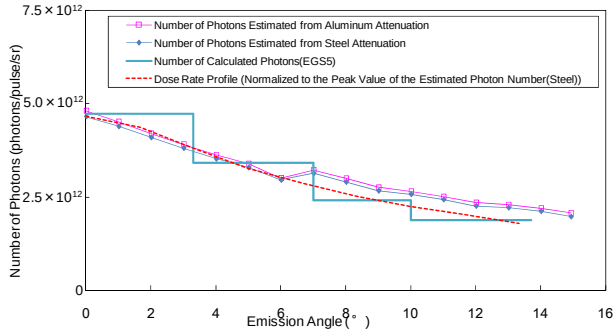

Fig. 10. Total photon number of 9MeV X-ray source for each emission angle.

A discontinuity in the measured angular distribution is surely recognized between emission angles of 6° and 7° in Fig. 9 and 10. This is thought to be due to insufficient structure of the multi-hole collimator which is placed in front of the detector array, because it has a segment structure around there and also all the measured curves show discontinuity.

We conclude that the angle and energy distributions of X-rays emitted from high power and high energy pulsed X-ray sources used for industrial CT can be measured accurately with the recently developed technique by utilizing thick aluminum attenuation material or steel attenuation material. Especially, it is a very important result for actual CT imaging that hardness of the energy spectrum can be measured quantitatively and it becomes dominant in forward angles in proportion to the energy of X-ray source.

This technique has a potential to become a standard method for measurement of energy spectra of in-

dustrially used X-ray sources. Finally, by utilizing information of the X-ray energy spectra obtained by the technique, the quality of obtained images will be improved in non-destructive industrial inspections such as X-ray CT.

4. CONCLUSION

A recently developed technique to measure X-ray energy spectra was extended for 6 MeV and 9 MeV X-ray sources used for industrial CT. To extend the applicable X-ray energy range we applied two different types of attenuation materials, one of which is relatively thicker aluminum for slow attenuation and the other is thinner steel for quick attenuation.

In this study, an attenuation curves are measured by using a step-shaped attenuation materials of aluminum and steel individually, and the each X-ray spectrum is reconstructed from the measured attenuation curve by the spectrum type Bayesian estimation method. In spite of obtained from independent measurement curve with individual attenuation material, it show quite similarity between energy spectra from aluminum attenuation curve and energy spectra from steel attenuation curve. Comparing with simulated spectra by the EGS5 code, the obtained X-ray energy spectra were confirmed to have good agreement except for higher energy region. Furthermore, this measuring technique derives measure two-dimensional (energy and angle dependent) spectra at one time. Precise measurement of the X-ray energy spectrum of high power and high energy pulsed X-ray sources more than 6 MeV was difficult in the past, but the presently expanded technique offers an easy standard X-ray energy spectrum measurement technique particularly for industrial X-ray sources.

The quality of X-ray CT image with high energy X-ray sources more than 6 MeV is expected to be improved for artifact-less by using the information on energy spectra obtained by the technique.

REFERENCES

1. Waggener RG, Blough MM, Terry JA, Chen D, Lee NE, Zhang S, McDavid WD. X-ray spectra estimation using attenuation measurement from 25 kVp to 18 MV. *Med. Phys*. 1999;26:1269-1278.
2. Iwasaki A, Kubota M, Hirota J, Fujimoto A, Suzuki K, Aoki M, Abe Y. Characteristic features of a high-energy x-ray spectra estimation method based on the Waggener iterative perturbation principle. *Med. Phys*. 2006;33:4056-4063.
3. Kanno I, Imamura R, Mikami K, Uesaka A, Hashimoto M, Ohtaka M, Ara K , Nomiya S, Onabe H. A current-mode detector for unfolding X-ray energy distribution. J. Nucl. Sci. Technol. 2008;45(11):1165-1170.
4. Takagi H, Murata I. Development of precise energy spectrum measurement technique for high power pulsed X-ray sources for industrial use. J. Nucl. Sci. Technol. 2016;53(6):766–773.
5. Hirayama H, Namito Y, Bielajew AF, Wilderman SJ, Nelson WR. The EGS5 code system. 2006;SLAC-R-730:1-436
6. Iwasaki S. A new approach for unfolding PHA problems based only on the Bayes' theorem. 9th International Symposium on Reactor Dosimetry. Prague Czech. September 2-6, 1996.
7. Takagi H, Terada Y, Murata I, Takahashi A. Measurement of double differential cross section of charged particle emission reactions by incident DT neutrons - correction for energy loss of charged particle in sample materials. Symposium on Nuclear Data. Tokai Japan. November 18-19, 1999.
8. Nauchi Y, et al. Measurements of hydrogen and helium isotopes emission spectra from neutrons induced reaction at ten's of MeV. Symposium on Nuclear Data. Tokai Japan. November 19-20, 1998.
9. Kondo K, Murata I, Ochiai K, Kubota N, Miyamaru H, Konno C, Nishitani T. Measurement and analysis of neutron-induced alpha particle emission double-differential cross section of carbon at 14.2MeV. J. Nucl. Sci. Technol. 2008;45: 103-115.
10. Nauchi Y, Iwasaki S. Convergence of unfolded spectrum with response function for single radiation based on Bayes' theorem. Nucl. Instrum. Methods. 2014;A735:437-443.